

Development and Demonstration of 12.4 GHz SiGe HBT Mixer for Radio over Fiber Applications

NORLIZA MOHAMED¹, SEVIA MAHDALIZA IDRUS², ABU BAKAR MOHAMMAD²,
SYAMSURI YAAKOB³

¹Razak School of Engineering and Advanced Technology,
UTM International Campus, Universiti Teknologi Malaysia,
Jalan Semarak, 54100 Kuala Lumpur, MALAYSIA.

²Photonic Technology Centre, Faculty of Electrical Engineering,
Universiti Teknologi Malaysia,
81310 Skudai, Johor Darul Takzim, MALAYSIA.

³Telekom Research and Development Sdn. Bhd.,
Lingkar Teknokrat Timur, 63000 Cyberjaya, Selangor, MALAYSIA.
Email: mnorliza@ic.utm.my¹

Abstract: – This work involves in conveying of an optically modulated intermediate frequency (IF) over fiber by employing the frequency up-conversion technique at the base station (BS), while the local oscillator (LO) signal was assumed to be remote and was located at the central station (CS). The main focus of this work is the development of optical front-end receiver for radio over fiber (RoF), whereby the LO signal was sent from CS to BS using the system. At the BS, the optically generated LO signal was used to up-convert the IF signal by using a microwave mixer. The mixer was developed utilizing heterojunction bipolar transistor (HBT) as its main active component due to the high internal gain offered and to allow the frequency conversion to take place. HBT mixer configuration was successfully modeled and simulated by employing harmonic-balance technique in Microwave Office (MWO) software. It has been verified through fabrication and device demonstration. In which, with the driven LO power of 0 dBm, the simulated conversion gain of -2.8 dB to 5.2 dB was obtained at -30 dBm to -10 dBm of IF input power level. The design was practically demonstrated and up-converted RF signal of up to 12.4 GHz was achieved.

Key-Words: – Frequency up-conversion, RF mixer, up-conversion mixer, SiGe heterojunction bipolar transistor (HBT), radio over fiber (RoF), harmonic balance technique, remote local oscillator.

1 Introduction

Currently, many works in RoF environment for mm-wave applications have been conducted and divulged. To realize mm-wave transmission system, appropriate techniques and configurations are required to adopt the mm-wave in any RoF system. There are many techniques that can be applied in generating the mm-wave signal either at the CS or at the BS itself depending on the requirements of the system. A lot of researchers have been studied to develop RoF architectures due to the importance of the mm-wave signal in most applications such as wireless system, radar system as well as software-defined radio. However, the generation of mm-wave signal with a frequency of tens of gigahertz is still a challenge for conventional electronics. Hence, many research activities have been carried out in generating the mm-wave signal optically, and the most common way to generate an mm-wave signal is to use optical heterodyne technique [1-3].

Additionally, there are three other state of the art techniques that have been investigated which are: external modulation [4-6], using optical transceiver [7-9] and frequency up- and down-conversion technique [10-12].

Frequency conversion techniques with integrated device has attracted high awareness in the RoF application whereby low IF signal can be transmitted from the CS to BS and minimize the fiber dispersion effect during the signal transmission. Moreover, the complexity and expensiveness of the BSs are avoided. An example to the technique is utilizing the electro-absorption modulator (EAM) integrated with semiconductor optical amplifier (SOA) module [13-15]. By using this technique, around 60 GHz of frequency up- and down-conversion of RF signal has been achieved. Some other techniques have been demonstrated by employing high electron mobility transistor (HEMT) [16-17], heterojunction photo-transistor

HPT [18-20], heterojunction bipolar transistor (HBT) [21-24], avalanche photodiodes (APDs) [25-27] and pin photodiodes (PDs) [28-30].

Generally, this paper proposes a front-end optical receiver for RoF system design with integrated heterojunction bipolar transistor (HBT) mixer. The proposed system is given in Fig. 1. RF mixer was designed to up-convert IF signal at 2.4 GHz to an RF signal of 12.4 GHz. The LO pumped signal was set to be at 10 GHz with pumping power in the range of -30 dBm to 30 dBm. The frequency up-conversion was intended to take place after both IF and LO optical signals were detected by the respective pin photodiode (PD). The pin PD converted the optical signals into the electrical signals before they were up-converted by the RF mixer. The up-converted signal was amplified using an electrical amplifier before it was transmitted to the end-users wirelessly.

Mainly, this paper is divided into several sections which are fundamental of RF mixing, the mixer design consideration, the design verification, HBT mixer model utilizing harmonic balance technique, device implementation and testing, results and discussion. Finally, the conclusion of this work is given in the last section.

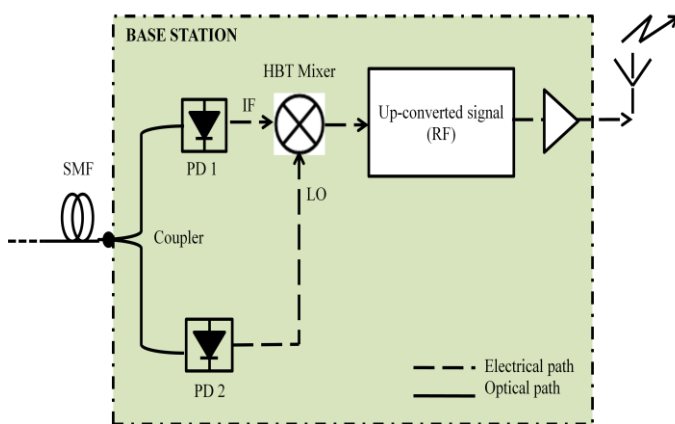


Fig. 1: Front-end optical receiver for RoF system with the proposed HBT up-conversion mixer.

2 Fundamental of RF Mixing

Theoretically, any nonlinear or rectifying device can be used as a mixer, however, only a few devices satisfy the practical requirements of mixer operation. Any device used as a mixer must have a strong nonlinearity, electrical properties that are uniform between individual devices, low noise, low distortion and adequate frequency response. A mixer basically has three ports consisting of a radio

frequency (RF) port, intermediate frequency (IF) port and local oscillator (LO) port.

The RF port is usually for the input signal where high frequency signal is applied while the IF port is for the output signal where the RF signal is modified by the LO signal. The LO is sometimes called the 'pump waveform' and it is required to pump the mixer. It is the port where the 'power' for the mixer is injected. LO signal is the strongest signal and is used to transform the RF frequency to the IF frequency or vice versa. Therefore, it can be said that the IF frequency at the output port is either up-converted or down-converted by the mixer when the LO is applied.

In this work, an up-conversion RF mixer was designed where IF signal was up-converted to an RF signal. Since IF frequency is usually smaller than RF frequency, therefore, whenever IF and RF are mentioned throughout the work in this paper, they will always referred to the input and output port respectively as shown in Fig.2.

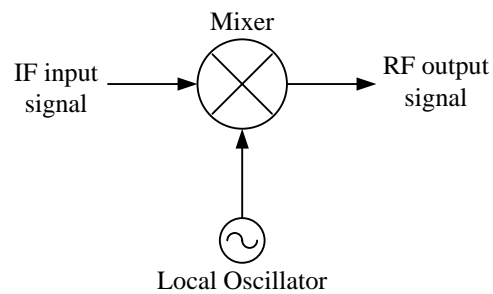


Fig. 2: A symbol of mixer used in this work.

Referring to Fig. 2, the output port of the mixer consists of frequencies that are given by:

$$f_{RF} = |\pm m f_{IF} \pm n f_{LO}| \quad (1)$$

Where f_{RF} , f_{IF} and f_{LO} are the frequencies of the RF, IF and LO respectively, while m and n are the harmonics integer of both IF and LO frequencies. In reality, the amplitude of the harmonic components decreases as the value of m and n increase. Mixer can be used to down-convert a frequency signal in a receiver or up-convert a frequency in a transmitter or exciter since it is a reciprocal device. However, in this work, the mixer is used at the receiver where the frequency is up-converted before transmitted wirelessly to the end users.

3 Mixer design consideration

In this work, SiGe BFP620 transistor in SOT343 package was chosen and the DC bias of the

transistor was determined. This transistor was chosen due to the availability of the discrete transistor in the market with the operating frequency in the point of interest. The DC biasing point was set to be at $V_{CE} = 2\text{ V}$, $I_C = 10\text{ mA}$ and in order to realize the desired operating point the following circuit design as in Fig. 3 was employed with 7.5 V DC bias voltage. From the simulation, $V_{CE} = 1.97\text{ V}$ and $I_C = 10.2\text{ mA}$ operating point were obtained.

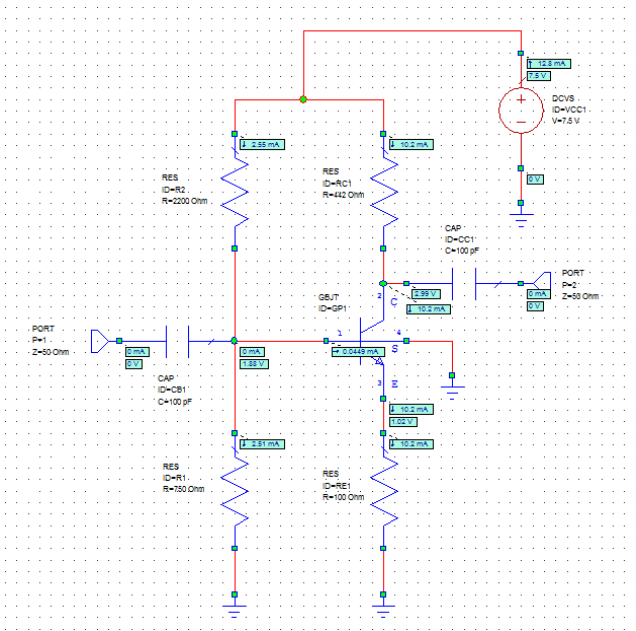


Fig. 3: DC bias circuit.

Scattering parameter, or normally known as S-parameter, is one of the crucial requirement in designing any circuit involving with active element such as a transistor. It is essential to determine the S-Parameter so that the maximum power transferred to the circuit, or also known as, circuit matching can be done appropriately. S-Parameters of BFP620 Transistor at $V_{CE} = 2\text{ V}$, $I_C = 10\text{ mA}$ that is used in this work have been provided by the manufacturer. In this work, we are only interested with the S- and Z-parameters at the desired frequencies, which are at the frequency of 2.4 GHz , 10 GHz and 12.4 GHz . Table 1 below summarized the S- and Z-parameters of the main RF mixer. Z-parameters were obtained from the S-parameters to perform the matching transformation.

To begin with, let us consider the input ports of the mixer. There are two ports that will be involved which are the IF port and the LO port. In designing both ports, the desired frequencies with their S-parameters should be considered. In order to perform the matching network of IF port, we would like to match the IF input impedance, $Z_{11\text{IF}} =$

$11.3525 + j 19.8552$ found in Table 1 with a $50\ \Omega$ matching impedance while in Fig. 4, it demonstrates the schematic of the selected IF matching network.

Table 1: S- and Z-parameters at the desired frequencies.

Frequency	2.4 GHz	10 GHz	12.4 GHz
S11	0.3524 / -154.2	0.523 / 71.4	0.68 / 44.7
S22	0.2618 / -79.4	0.2419 / 93.7	0.4379 / 61
Z11	$11.3525 + j 19.8552$	$148.273 + j96.0895$	$174.015 - j25.8995$
Z22	$35.5557 + j14.2339$	$152.386 + j30.1641$	$116.287 - j72.1678$

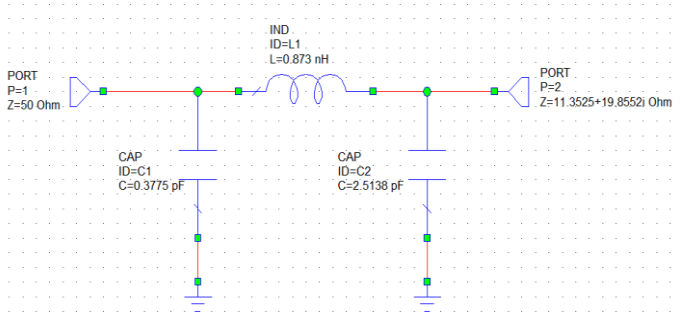


Fig. 4: IF Matching Network

Similarly for the LO port, we would like to match the LO input impedance, $Z_{11\text{LO}} = 148.273 + j96.0895$ that is also found in Table 1 with a $50\ \Omega$ matching impedance. The following Fig. 5 depicts the schematic of the LO matching network. For the output matching, we will consider the load or output impedance instead of the input impedance of the RF port. Therefore, we transformed a $50\ \Omega$ to match to the RF load impedance, $Z_{22\text{RF}} = 116.287 - j72.1678$ as obtained in Table 1. The schematic that is required to achieve the RF matching is shown in Fig. 6.

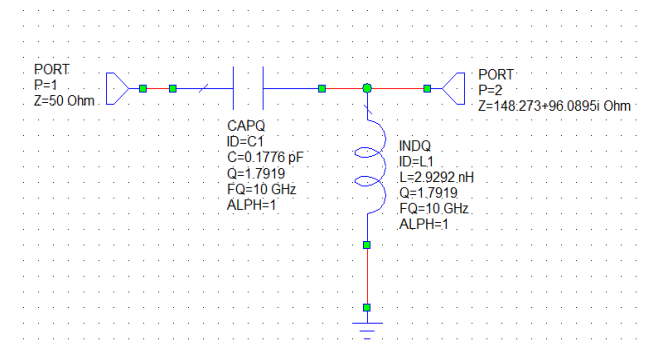


Fig. 5: LO Matching Network

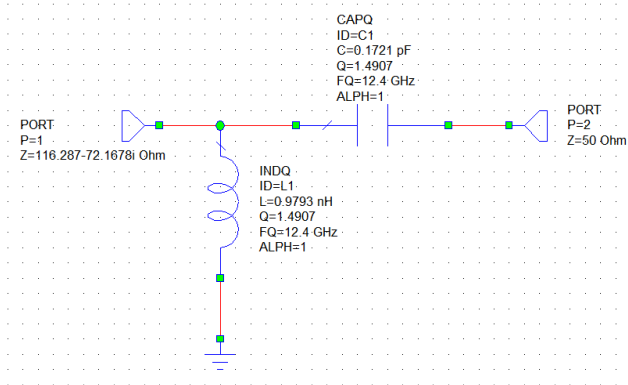


Fig. 6: RF Matching Network

In this impedance matching design, we assumed that the transistor was to be operating in a quasi-linear mode, whereby, to produce the mixing effect, the transistor has to be nonlinear. In addition, the linearity was small enough with the intention that usual linear procedure and concept of impedance can be applied and this is usually a valid assumption.

4 Design verification

Generally, in order to have a proper impedance matching circuits at both input and output ports, we firstly considered the return loss (S11) and power gain (S21) at each port. For a better performance and closely match to the real environment, all the designs were simulated using EM (electromagnetic) simulator. It is software that usually used for passive circuit analysis. Fig. 7 illustrates the IF matching structure using EM simulator followed by its return loss which is depicted in Fig. 8. It is shown that the return loss dropped about -41.54 dB at 2.4 GHz.

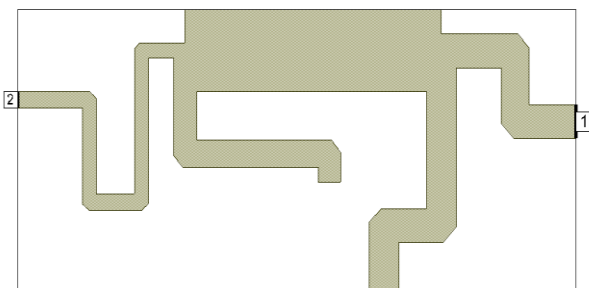


Fig. 7: IF matching structure using EM simulator.

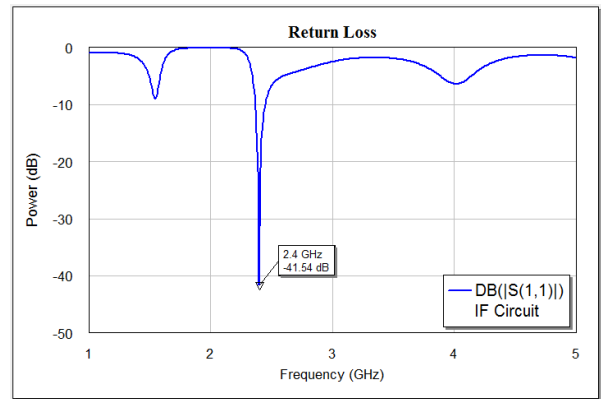


Figure 8: Return loss of the IF matching structure.

For the LO matching structure using EM simulator, it can be described in Fig. 9. Its return loss fell at about -24.58 dB for the frequency of 10 GHz. The graph can be observed in Fig. 10.

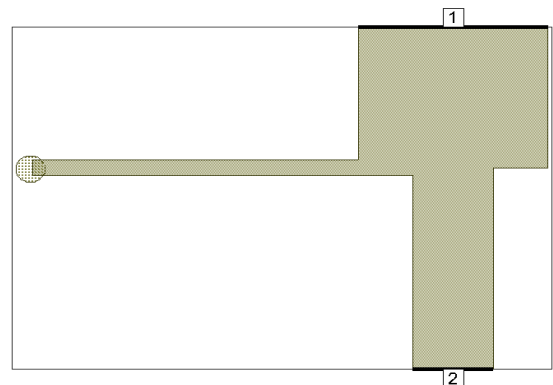


Fig. 9: LO matching structure using EM simulator.

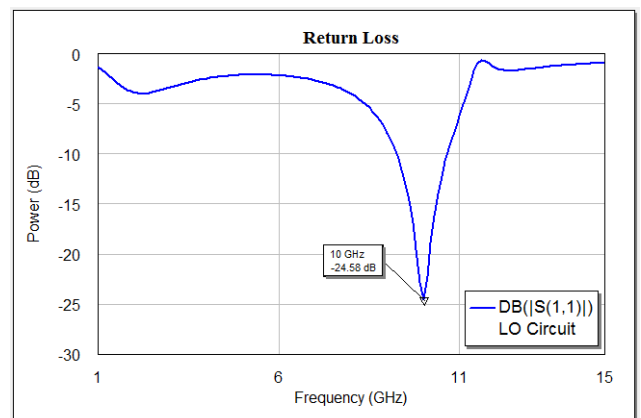


Fig. 10: Return loss of the LO matching structure.

In Fig. 11, it demonstrates the RF matching structure using EM simulator. Its return loss is depicted in Fig. 12 and it revealed that the return loss dropped at -51.1 dB for frequency of 12.4 GHz.

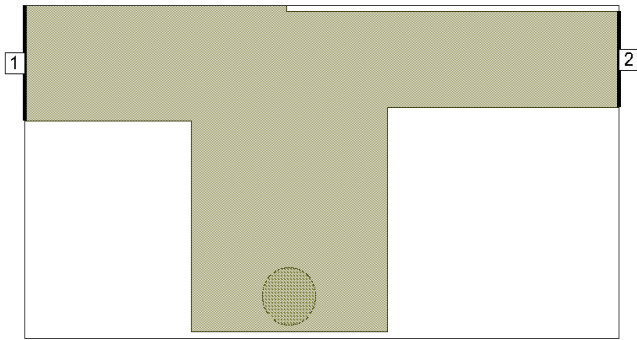


Fig. 11: RF matching structure using EM simulator.

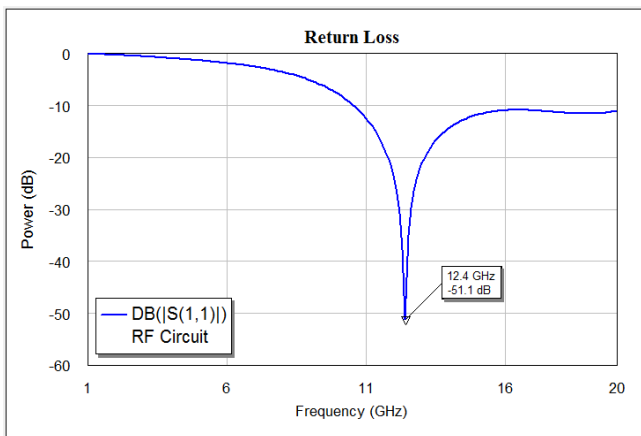


Fig. 12: Return loss of the RF matching structure.

5 HBT mixer model

Before detail description of the mixer modeling is presented, first, fundamental of harmonic balance technique will be explained. There are few difficulties in a time-domain approaches. Firstly, the circuit might contain an input and output impedance matching network, signal filters and frequency-dependent transistor parameters such as the base transport factor. Secondly, since in the current investigation only the steady-state solution of the maxing is of interest, the number of local oscillator (LO) cycles that the simulator takes to reach a steady state can be very high. Finally and most importantly, not only the LO frequency that is involves during the mixing but IF, other up- and down-converted frequencies and image frequencies will also involve.

Harmonic balance allows the linear parts of the model to be described and simulated in the frequency domain and the nonlinear parts in the time-domain, and forward and inverse Fourier transforms are used to bridge the two parts. Therefore the problem describing the responses of

the linear elements in the time-domain is avoided. Also harmonic balance attempts to find the steady-state solution from the outset and hence no time is wasted on the transient. Since the mixer is analysed separately for the LO and photo-generated IF signal excitations, thus the number of simulation points and the computation time will be independent of the frequency relationship between the LO, IF and radio frequency (RF).

In conventional large signal analysis, the nonlinear components must be modeled in the time-domain. At the same time, the reactive elements can no longer be described by their complex phasors but must be specified with their time-dependent differential equations. Simulation is carried out for a number of LO cycles until a steady state is reached which is usually controlled by the reactive elements. The situation is different if harmonics balance techniques are used.

The concept of the harmonic balance techniques can be illustrated with Fig. 13. As seen in the figure, the circuit is partitioned in two sub networks; one that contains all the linear elements and another that encompasses the nonlinear devices. The voltage at interconnecting ports are considered as the unknowns, so the goal of harmonic balance analysis is to find the set voltage phasors in such a way that Kirchoff's laws are satisfied to desired accuracy.

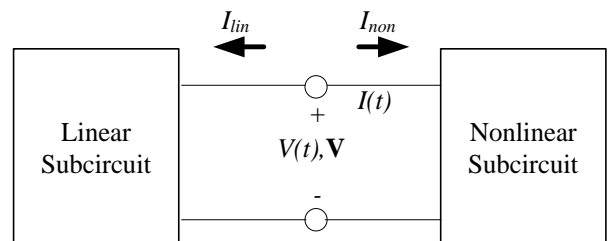


Fig. 13: The concept of harmonic balance technique.

Any large-signal equivalent circuit consists of linear (ideal R, C) and nonlinear (*p-n* junction). In small-signal analysis, the nonlinear elements are linearized around the DC bias point so that their differential resistances or conductance's can be treated as if they were linear. Nonlinear sub-circuit is described in time domain whereas, LO is embedded in the linear sub-circuit as an AC voltage source at LO frequency, f_{LO} .

$$I(t) = f(V(t)) \tag{2}$$

Where,

$V(t)$ – instantaneous terminal voltage across both the linear and nonlinear subcircuits.

$I(t)$ – corresponding current flowing into nonlinear subcircuit

The main difference between harmonic balance and transient analysis is that the harmonic balance approach uses a linear combination of sinusoids to build the solution. Thus, it approximates naturally the periodic and quasi-periodic signals found in a steady-state response. Harmonic balance also differs from traditional time domain methods in that, time domain simulators represent waveforms as a collection of samples, whereas harmonic balance represents them using coefficients of sinusoids. Harmonic balance converts the coefficient representation of the stimulus into a sampled data representation; this is a conversion from the frequency domain to the time domain, which can be accomplished by the inverse Fourier transforms. With this representation, the nonlinear devices are easily evaluated. The results are then converted back into coefficient form using the Fourier transform.

The harmonic balance method has gained widespread acceptance among microwave engineers as a simulation tool for nonlinear circuits. The main advantages of this approach are its ability to directly address the steady state circuit operation under single or multiple tone excitations, and its compatibility with the characterization of the linear sub-network in the frequency domain for high frequency application. There are a number of commercial harmonic balance simulators available for nonlinear microwave circuits' simulation, while the Microwave Office simulator was chosen for this work.

The mixing mechanism in an HBT arises from the two internal pn junction since these two junctions exhibit nonlinear exponential current-voltage characteristics. For example, when two voltages v_1 and v_2 are at frequencies f_1 and f_2 , respectively, appear across the forward-biased base-emitter junction, the junction will conduct a current which contains components at frequency $|nf_1 \pm mf_2|$ where n and m are any integers. These current components will in turn cause other voltage components at the same frequencies to appear across the junction through the linear parts of the circuit, such as any resistance and capacitance, and hence the mixing continues. This description of the mixing mechanisms is very general and often computer modeling for a mixer is closely linked to such a description.

To develop the HBT mixer circuit model, it is required to consider several stages of works including the parameter settings, transistor data collection and characterization, and determination of

board properties. All the considerations will be put into account during the simulation of the circuit model.

The following Table 2 shows the parameter settings for the HBT mixer circuit model used for the simulation. While in Table 3, it describes the data settings for BFP620 transistor used in the mixer circuit model. These data were obtained from the datasheet provided by the manufacturer. For the simulation, it is also essential to include the properties of the board being employed. RO3003 board from Rogers Corporation was chosen due to the capability of the board to be operating at high frequency ranges. The properties of the board can be seen in Table 4.

Table 2: Parameters setting of HBT mixer circuit model.

Symbol	Value	Description
IF Port	$f_{IF} = 2.4$ GHz -30 dBm < P_{IF} < 0 dBm	Frequency and power set at IF input port (Port 1)
LO Port	$f_{LO} = 10$ GHz -30 dBm < P_{LO} < 30 dBm	Frequency and power set at LO input port (Port 2)
R_1	750 Ω	Base resistance 1
R_2	2200 Ω	Base resistance 2
R_C	442 Ω	Collector resistance
R_E	100 Ω	Emitter resistance
C_1	3.979 pF	IF capacitance 1
C_2	6.641 pF	IF capacitance 2
C_3	0.1776 pF	LO capacitance
C_4	0.1721 pF	RF capacitance
C_C	100 pF	Collector DC block
C_B	100 pF	Base DC block
L_1	1.945 nH	IF inductance
L_2	2.929 nH	LO inductance
L_3	0.9793 nH	RF inductance
VCC	7.5 V	DC Voltage supply

6 Device implementation

The circuit implementation will be specifically described in this section. The circuit model of the mixer is depicted in Fig. 14 which shows the circuit model in its lumped elements form. It consists of three ports which are IF and LO ports as the input ports and RF port as the output port. LO power must be higher than IF power since it acts as a driver or pumping signal to control the switching of the mixer.

For high frequency circuits, simulation in distributed circuit, or also known as, transmission line circuit, is more preferable since it is more

accurate whereby all parameters such as tangent loss, dielectric constant, and height and thickness of the board were considered during simulation. Since this circuit came across the frequency of up to 12.4 GHz, thus, the transmission line circuit was employed. In this work Roger board RO3003 was employed with the characteristics that have been described in Table 4.

Table 3: Data setting of BFP620 Transistor.

Symbol	Value	Description
C_{cb}	0.12 pF	Collector-base capacitance
C_{ce}	0.22 pF	Collector-emitter capacitance
C_{eb}	0.46 pF	Emitter-base capacitance
I_s	0.22 fA	Saturation current
I_{se}	21 fA	BE leakage current parameter
I_{sc}	18 pA	BC leakage current parameter
B_f	425	Forward current gain
B_r	50	Reverse current gain
N_f	1.025	Forward ideality factor
N_r	1.0	Reverse ideality factor
t_f	1.43 ps	Forward transit time
t_r	0.2 ns	Reverse transit time

Table 4: Properties of RO3003 Roger Board

Symbol	Value	Description
ϵ_r	3	Relative dielectric constant
δ	0.0013	Tangent loss or dissipation factor of the dielectric
H	0.762 mm	Height of the substrate
T	35 μ m	Thickness of the conductor

From schematic diagram of Fig. 14, hence the layout of the mixer can be obtained. The layout file was then be edited and converted into AutoCad file for hardware translation. The physical layout drawing of the HBT mixer for both front and back views can be seen in Fig. 15 (a) and (b) respectively. Next, Figure 16 demonstrates the HBT mixer board connection and testing for frequency up-conversion at 12.4 GHz.

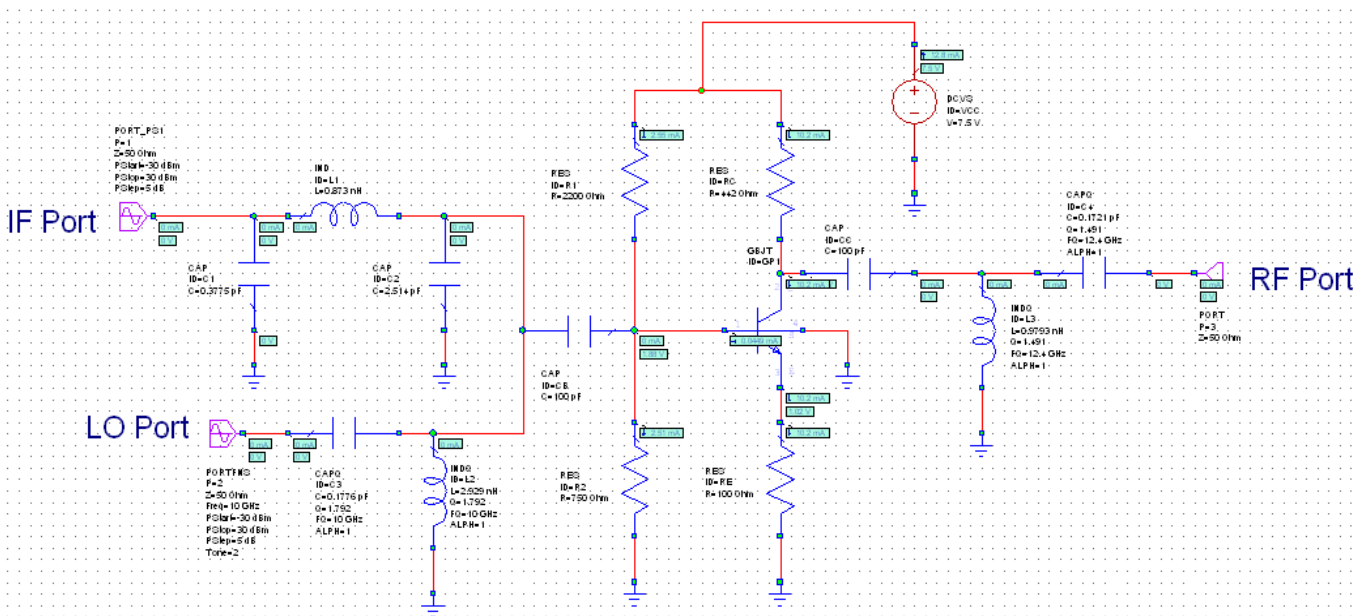
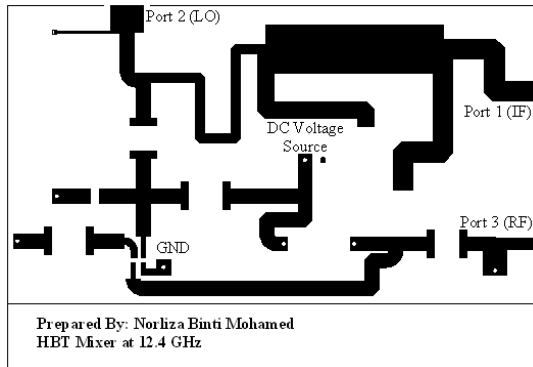
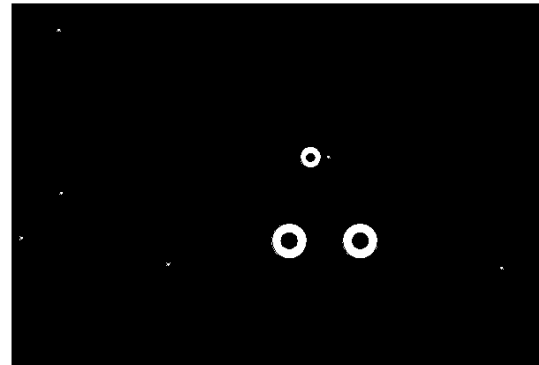


Figure 14: Schematic diagram of the lumped element circuit model.



(a)



(b)

Fig. 15: Physical Layout of HBT Mixer: (a) Front view, (b) Back view.

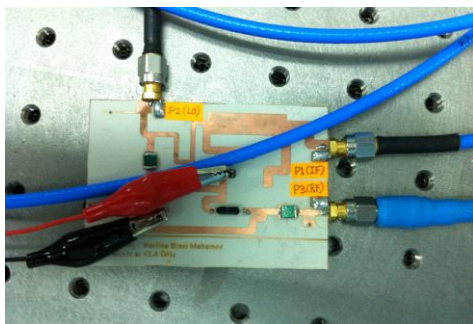


Figure 16: Board connection and testing.

7 Results and discussion

At the output port, RF output spectrum obtained from the simulation can be seen in Fig. 17. The power level for both inputs i.e. IF power level at 2.4 GHz and LO power level at 10 GHz were set at -10 dBm and 4 dBm respectively. From the graph it was found that the power level at 12.4 GHz was achieved at about -29 dBm. Whilst, the following Fig. 18 shows the RF output spectrum at 12.4 GHz obtained from the measurement. IF and LO input power levels were set at -10 dBm and 0 dBm respectively.

Based on the output power level, the conversion loss of the mixer from the simulation and measurement can be found in Fig. 19 and 20 in the function of different IF and LO power levels respectively. From the graphs, we obtained the conversion loss about -2.6 dB to 5.2 dB at about -30 dBm to -10 dBm of IF input power level.

As can be seen, at LO power level of 0 dBm the conversion loss occurred at IF power level from -30 dBm until it reached about -23 dBm where the conversion gain started. The conversion gain kept on rising until the IF power level reached about -5 dBm and then the conversion gain started to decrease slowly.

The comparison of this work with the previous reported works can be seen in Table 5. The table shows the conversion gain obtained from this work as compared to the other work but at different LO power level and frequency settings.

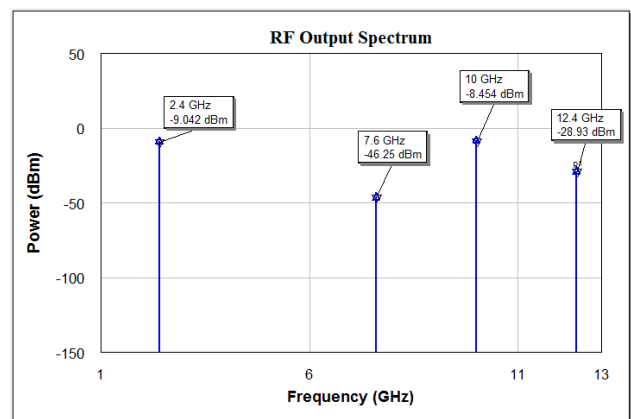


Fig. 17: Simulated RF output spectrum at 12.4 GHz.

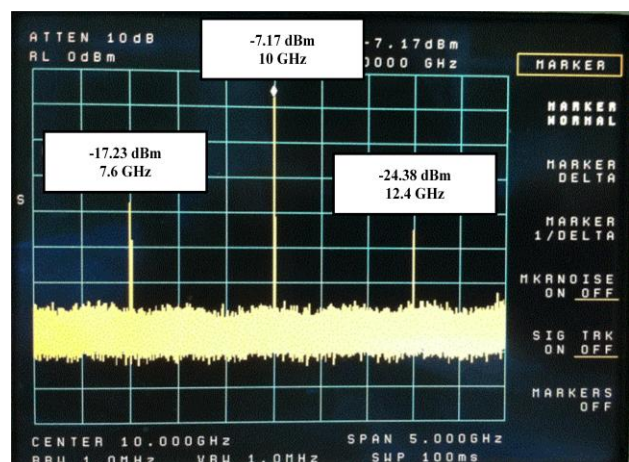


Figure 18: Measured RF output spectrum at 12.4 GHz.

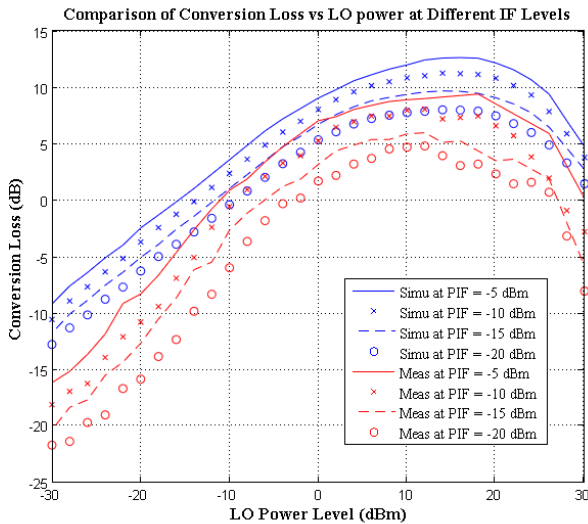


Fig. 19: Comparison between simulation and measurement of conversion loss at different IF level.

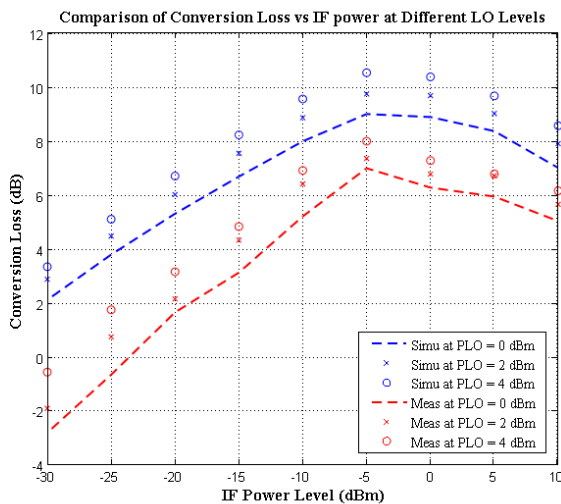


Fig. 20: Comparison between simulation and measurement of conversion loss at different LO level.

8 Conclusion

In this work, we have developed an RF mixer utilizing HBT as its main active component which located at the BS. The mixer has shown a practical performance with the conversion gain of 5.2 dB at -10 dBm of modulated IF power level and 0 dBm of LO pumped power. The design was practically demonstrated and up-converted RF signal of up to 12.4 GHz was achieved. Presently, we are developing an up-conversion design for frequency of up to 42.4 GHz. As for now, we have conducted the simulation and managed to achieve an up-

conversion frequency in the millimeter-wave band. The results will be demonstrated with this configuration for future practical development millimeter-wave radio over fiber system.

Table 5: Previous reported works specifically based on HBT configurations.

Config./Tech.	Freq. [GHz]	Conv. Gain [dB]	LO Power [dBm]	Ref.
SiGe HBT	$f_{IF} = 1.25$ $f_{RF} = 28$	1	NA	Comeau <i>et al.</i> [22] (2006)
SiGe HBT	$f_{IF} = 0.02$ $f_{LO} = 5.8$ $f_{RF} = 4.9$	4.2	-3	Myoung <i>et al.</i> [21] (2006)
GaAs HBT	$f_{IF} = 0.22$ $f_{LO} = 4.68$ $f_{RF} = 4.9$	3.7	-14	Jung <i>et al.</i> [24] (2005)
GaAs HBT	$f_{IF} = 1.8$ $f_{LO} = 22.2$ $f_{RF} = 24$	4	4.2	Huber <i>et al.</i> [23] (2005)
SiGe HBT	$f_{IF} = 2.4$ $f_{LO} = 10$ $f_{RF} = 12.4$	5.2	0	This Work

Acknowledgement: – The authors acknowledge the Ministry of Higher Education (MOHE) Malaysia and Universiti Teknologi Malaysia (UTM) for the supports and scholarship of doctoral study. They also acknowledge Telekom Malaysia Research and Development (TMR&D) Cyberjaya, for the lab facilities.

References:

- [1] C. Xiangfei, *et al.*, "Photonic generation of microwave signal using a dual-wavelength single-longitudinal-mode fiber ring laser," *Microwave Theory and Techniques, IEEE Transactions on*, vol. 54, pp. 804-809, 2006.
- [2] T. Kuri and K. Kitayama, "Optical heterodyne detection technique for densely multiplexed millimeter-wave-band radio-on-fiber systems," *Lightwave Technology, Journal of*, vol. 21, pp. 3167-3179, 2003.
- [3] R. Hofstetter, *et al.*, "Dispersion effects in optical millimeter-wave systems using self-heterodyne method for transport and generation," *Microwave Theory and*

- Techniques, IEEE Transactions on*, vol. 43, pp. 2263-2269, 1995.
- [4] Q. Guohua, *et al.*, "Generation and distribution of a wide-band continuously tunable millimeter-wave signal with an optical external modulation technique," *Microwave Theory and Techniques, IEEE Transactions on*, vol. 53, pp. 3090-3097, 2005.
- [5] T. Kuri, *et al.*, "Fiber-optic millimeter-wave downlink system using 60 GHz-band external modulation," *Lightwave Technology, Journal of*, vol. 17, pp. 799-806, 1999.
- [6] G. H. Smith, *et al.*, "Technique for optical SSB generation to overcome dispersion penalties in fibre-radio systems," *Electronics Letters*, vol. 33, pp. 74-75, 1997.
- [7] K. Kitayama, *et al.*, "Full-duplex demonstration of single electroabsorption transceiver basestation for mm-wave fiber-radio systems," in *Microwave Photonics, 2001. MWP '01. 2001 International Topical Meeting on*, 2002, pp. 73-76.
- [8] T. Kuri, *et al.*, "60 GHz band full-duplex radio-on-fiber system using two-port electroabsorption transceiver," *IEEE Photonics Technology Letter*, vol. 12, pp. 419-421, April 2000 2000.
- [9] K. Kitayama, *et al.*, "An approach to single optical component antenna base stations for broad-band millimeter-wave fiber-radio access systems," *Microwave Theory and Techniques, IEEE Transactions on*, vol. 48, pp. 2588-2595, 2000.
- [10] S. M. Idrus, *et al.*, "Harmonic Balance Analysis of the Downconversion Optoelectronic Mixer in HBT Photodetector," presented at the Regional Annual Fundamental Science Seminar (RAFSS) and 2nd International Conference on Mathematical Sciences (ICoMS), Johor Bahru, Malaysia, 2007.
- [11] K. I. Kitayana and R. A. Griffin, "Optical downconversion from millimeter-wave to IF-band over 50 km-long optical fiber link using an electroabsorption modulator," *Photonics Technology Letters, IEEE*, vol. 11, pp. 287-289, 1999.
- [12] G. H. Smith and D. Novak, "Broadband millimeter-wave fibre-radio network incorporating remote up/down-conversion," *IEEE MTT-S International Microwave Symposium*, vol. 3, pp. 1509-1512, 1998.
- [13] K. Hyung-Jun and S. Jong-In, "Analog performance of an all-optical frequency upconverter utilizing an electro-absorption modulator for radio-over-fiber applications," in *Microwave and Millimeter Wave Technology (ICMMT), 2010 International Conference on*, 2010, pp. 1575-1577.
- [14] H. J. Kim and J. I. Song, "Photonic frequency upconversion technique using electro-absorption modulator for radio-over-fibre applications," *Electronics Letters*, vol. 46, pp. 1512-1513, 2010.
- [15] J.-H. Seo, *et al.*, "SOA-EAM Frequency Up/Down-Converters for 60-GHz Bi-Directional Radio-on-Fiber Systems," *IEEE Transactions on Microwave Theory & Tech.*, vol. 54, February 2006 2006.
- [16] C. Chang-Soon and C. Woo-Young, "Millimeter-wave optoelectronic mixers based on InP HEMT," in *The 17th Annual Meeting of the IEEE Lasers and Electro-Optics Society*, 2004, pp. 126-127 Vol.1.
- [17] C. Chang-Soon, *et al.*, "Phototransistors based on InP HEMTs and their applications to millimeter-wave radio-on-fiber systems," *IEEE Transactions on Microwave Theory and Techniques*, vol. 53, pp. 256-263, 2005.
- [18] J. Y. Kim, *et al.*, "Characteristics of InP-InGaAs HPT-Based Optically Injection-Locked Self-Oscillating Optoelectronic Mixers and Their Influence on Radio-Over-Fiber System Performance," *Photonics Technology Letters, IEEE*, vol. 19, pp. 155-157, 2007.
- [19] K. Jae-Young, *et al.*, "60 GHz radio-on-fiber downlink systems using optically injection-locked self-oscillating optoelectronic mixers based on InP/InGaAs HPTs," in *Optical Fiber Communication Conference. OFC 2006*, 2006, p. 3 pp.
- [20] C. Chang-Soon, *et al.*, "Optically injection-locked self-oscillating optoelectronic mixers based on InP-InGaAs HPTs for radio-on-fiber applications," *Photonics Technology Letters, IEEE*, vol. 17, pp. 2415-2417, 2005.
- [21] M. No Gil, *et al.*, "A low voltage SiGe HBT up-conversion mixer for 5.8 GHz WLAN," in *Radio and Wireless Symposium, 2006 IEEE*, 2006, pp. 435-438.
- [22] J. P. Comeau and J. D. Cressler, "A 28-GHz SiGe up-conversion mixer using a series-connected triplet for higher dynamic range and improved IF port return loss," *Solid-State Circuits, IEEE Journal of*, vol. 41, pp. 560-565, 2006.
- [23] M. Huber, *et al.*, "Ultra low power 24 GHz HBT mixer," in *Microwave and Optoelectronics, 2005 SBMO/IEEE MTT-S International Conference on*, 2005, pp. 24-27.

- [24] J. Joo-Yong, *et al.*, "High linear single-ended up-conversion mixer using InGaP/GaAs HBT process," in *Microwave Conference Proceedings, 2005. APMC 2005. Asia-Pacific Conference Proceedings, 2005*, p. 4 pp.
- [25] L. Myung-Jae, *et al.*, "Fiber-fed 60-GHz self-heterodyne system using a self-oscillating harmonic optoelectronic mixer based on a CMOS-compatible APD," in *IEEE MTT-S International Microwave Symposium Digest, 2008*, pp. 587-590.
- [26] L. Myung-Jae, *et al.*, "Self-Oscillating Harmonic Opto-Electronic Mixer Based on a CMOS-Compatible Avalanche Photodetector for Fiber-Fed 60-GHz Self-Heterodyne Systems," *Microwave Theory and Techniques, IEEE Transactions on*, vol. 56, pp. 3180-3187, 2008.
- [27] K. Hyo-Soon and C. Woo-Young, "CMOS-compatible 60 GHz Harmonic Optoelectronic Mixer," in *IEEE/MTT-S International Microwave Symposium.*, 2007, pp. 233-236.
- [28] S. A. Malyshev and A. L. Chizh, "p-i-n Photodiodes for Frequency Mixing in Radio-Over-Fiber Systems," *Journal of Lightwave Technology*, vol. 25, pp. 3236-3243, 2007.
- [29] S. A. Malyshev and A. L. Chizh, "Optoelectronic mixer for radio-on-fiber systems," in *Microwave Conference, 2005 European*, 2005, p. 4 pp.
- [30] H. Ogawa and Y. Kamiya, "Fiber-optic microwave transmission using harmonic laser mixing, optoelectronic mixing, and optically pumped mixing," *Microwave Theory and Techniques, IEEE Transactions on*, vol. 39, pp. 2045-2051, 1991.